Supplementary information for

Core-Shell Heterostructured CuFe@NiFe Prussian Blue Analogue as A Novel Electrode Material for High-Capacity and Stable Capacitive Deionization

Yubo Zhao, [ab] Bolong Liang, [ab] Xujie Wei, [ab] Kexun Li, [*ab] and Cuicui Lv [*ab], Yong Zhao [c]

[a] The College of Environmental Science and Engineering, Nankai University, Tianjin 300071, China

[b] MOE Key Laboratory of Pollution Processes and Environmental Criteria, Tianjin Key Laboratory of Environmental Remediation and Pollution Control, Tianjin Key Laboratory of Environmental Technology for Complex Trans-Media Pollution, Nankai University, Tianjin 300071, China

[c] State Key Laboratory of Simulation and Regulation of Water Cycle in River Basin, China Institute of Water Resources and Hydropower Research, Beijing 100038, China

*** Corresponding author.**

E-mail addresses: likx@nankai.edu.cn (K. Li), lvcuicui870818@163.com (C. Lv).

Materials and methods

2.1. Material synthesis and electrode fabrication

The synthetic procedure of NiFe PBA was similar to that of CuFe PBA. 3.8 mM $NiCl_2 \cdot 6H_2O$ solution and 4.2 mM $K_3Fe(CN)_6$ solution with an equal volume of 200 mL were simultaneously added drop-wise to 200 mL of deionized water under vigorously stirring. After complete addition, the mixed solution was continually stirred for 12h and subsequently aged for 12h. The obtained precipitates were centrifuged and washed for several times, and finally dried overnight at 60 °C.

The electrode fabrication steps for NiFe PBA stayed unchanged with those for CuFe PBA and CuFe@NiFe PBA.

(a)

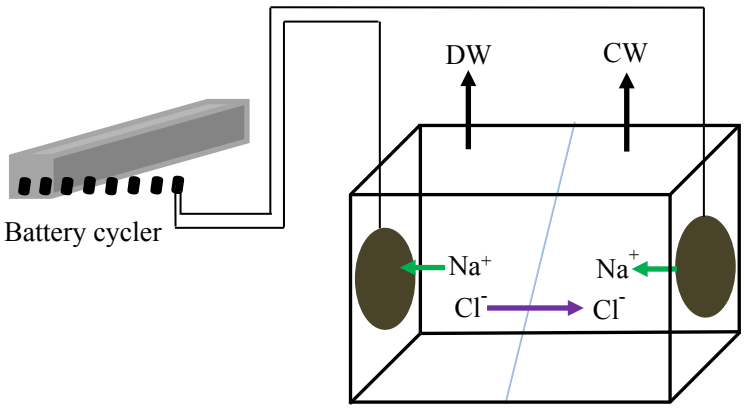

(b)

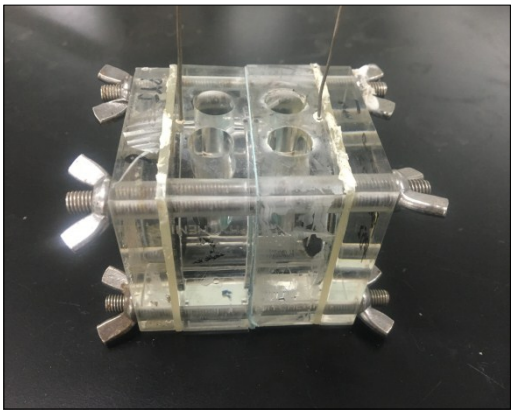

Fig. S1 Schematic diagram of the CDI cell (a); A photo of the CDI cell (b).

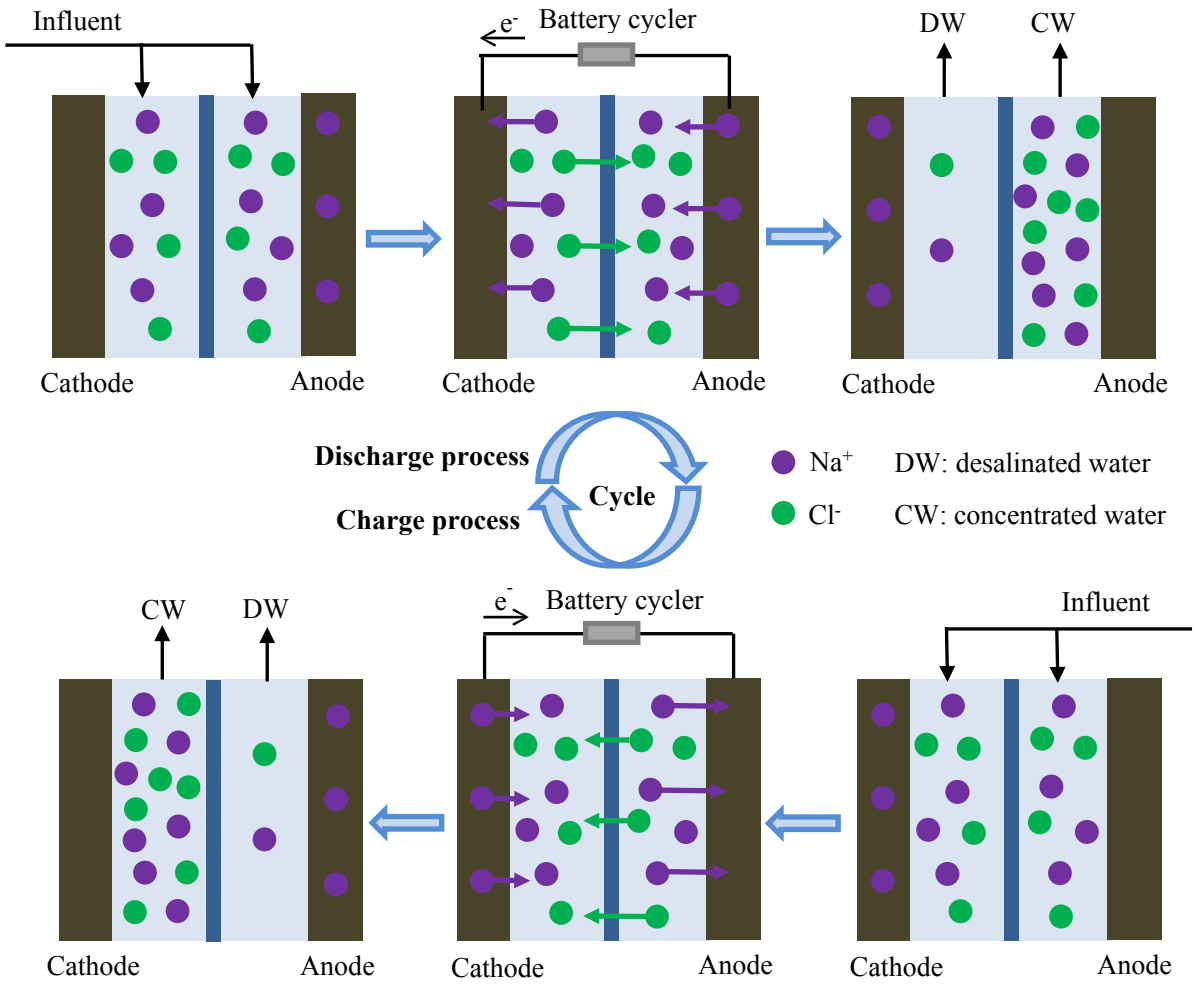

Fig. S2. Desalination tests via the two-chamber CDI cell during a cycle.

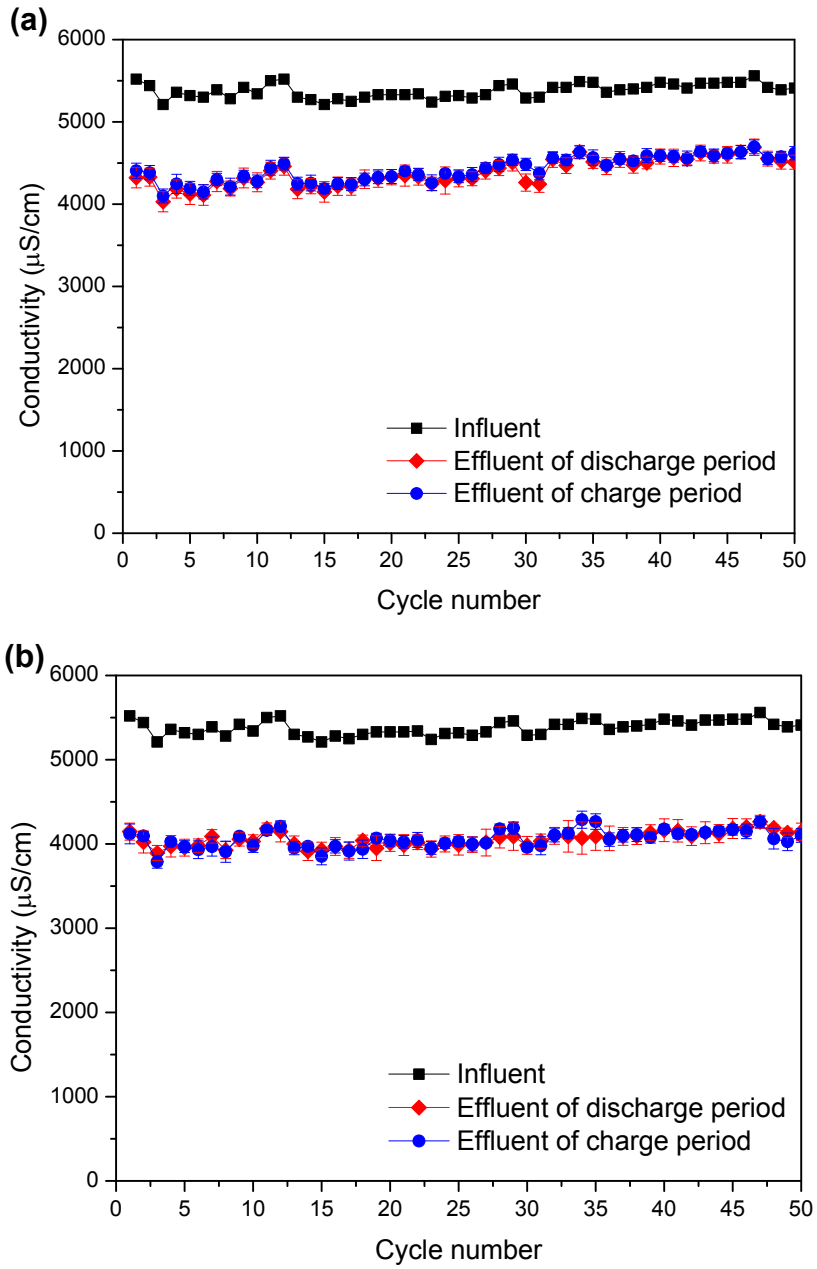

Fig. S3. The conductivities of influent and effluent for CuFe PBA cell (a) and CuFe@NiFe PBA cell (b).

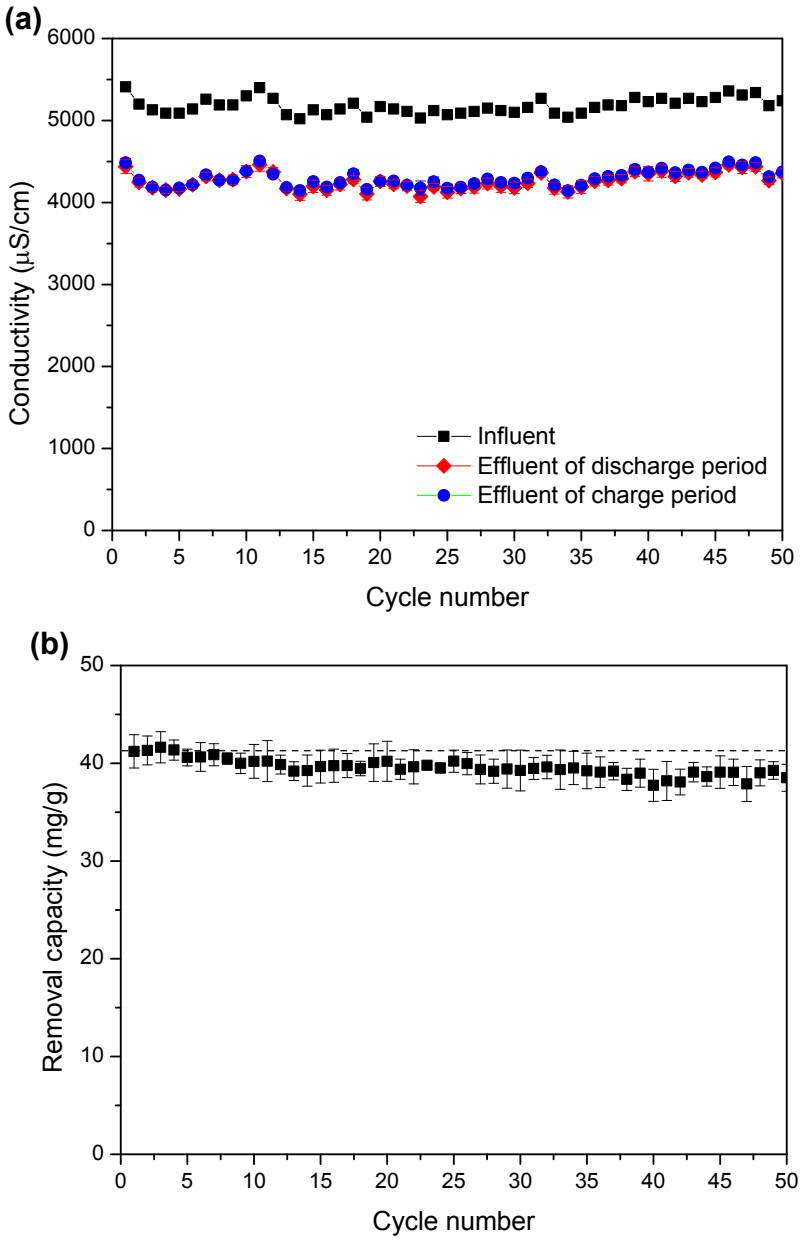

Fig. S4. The conductivities of influent and effluent for NiFe PBA cell (a); Desalination recyclability of NiFe PBA cell (b).

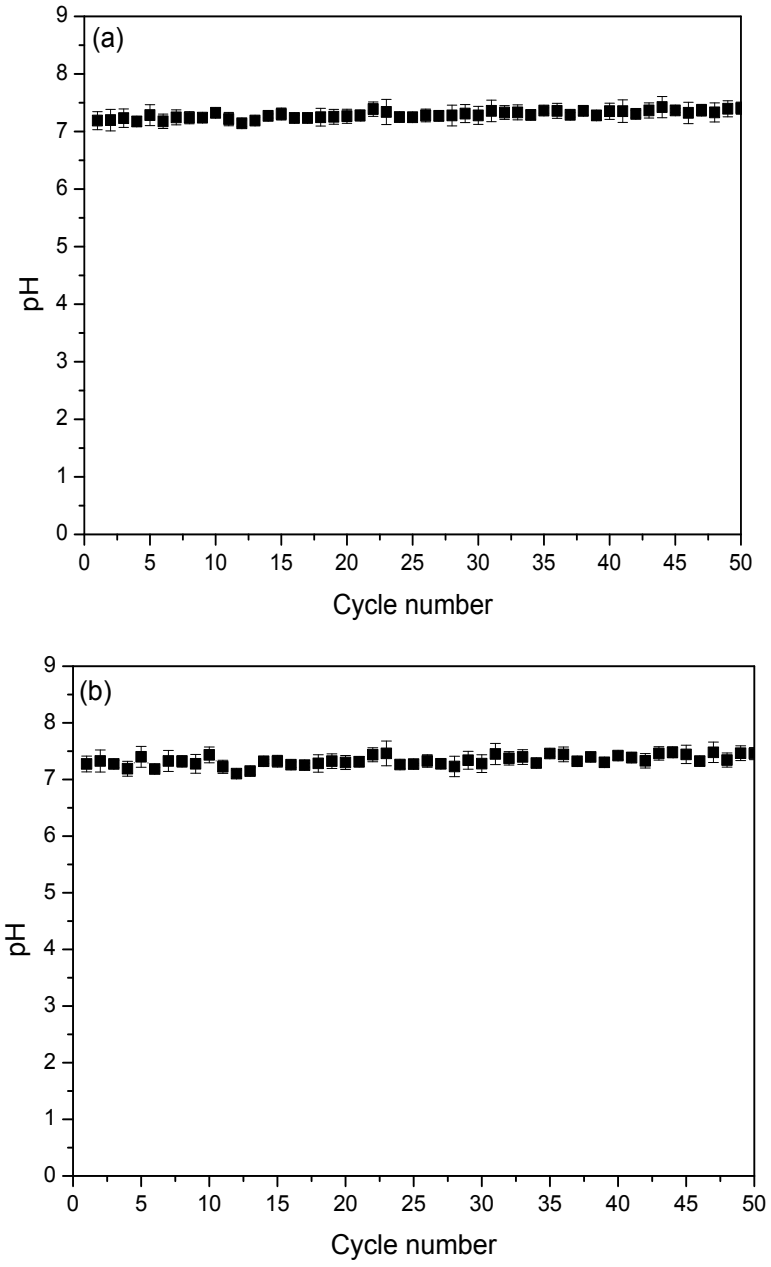

Fig. S5. The effluent pH of CuFe PBA cell (a) and CuFe@NiFe PBA cell (b).

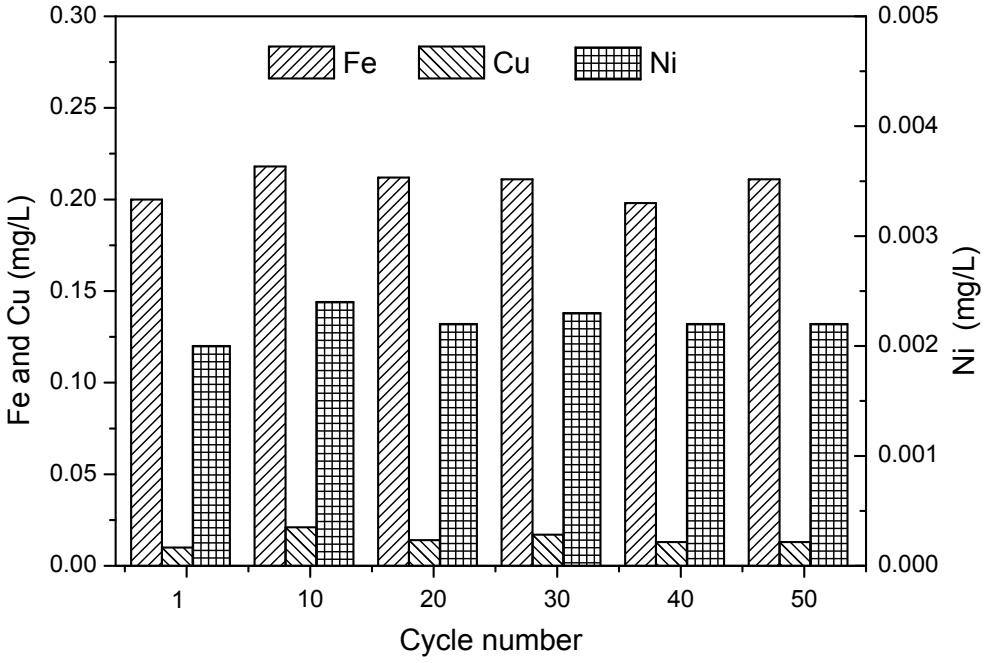

Fig. S6. Concentrations of Fe, Cu and Ni ions in the effluent of CuFe@NiFe PBA cell.

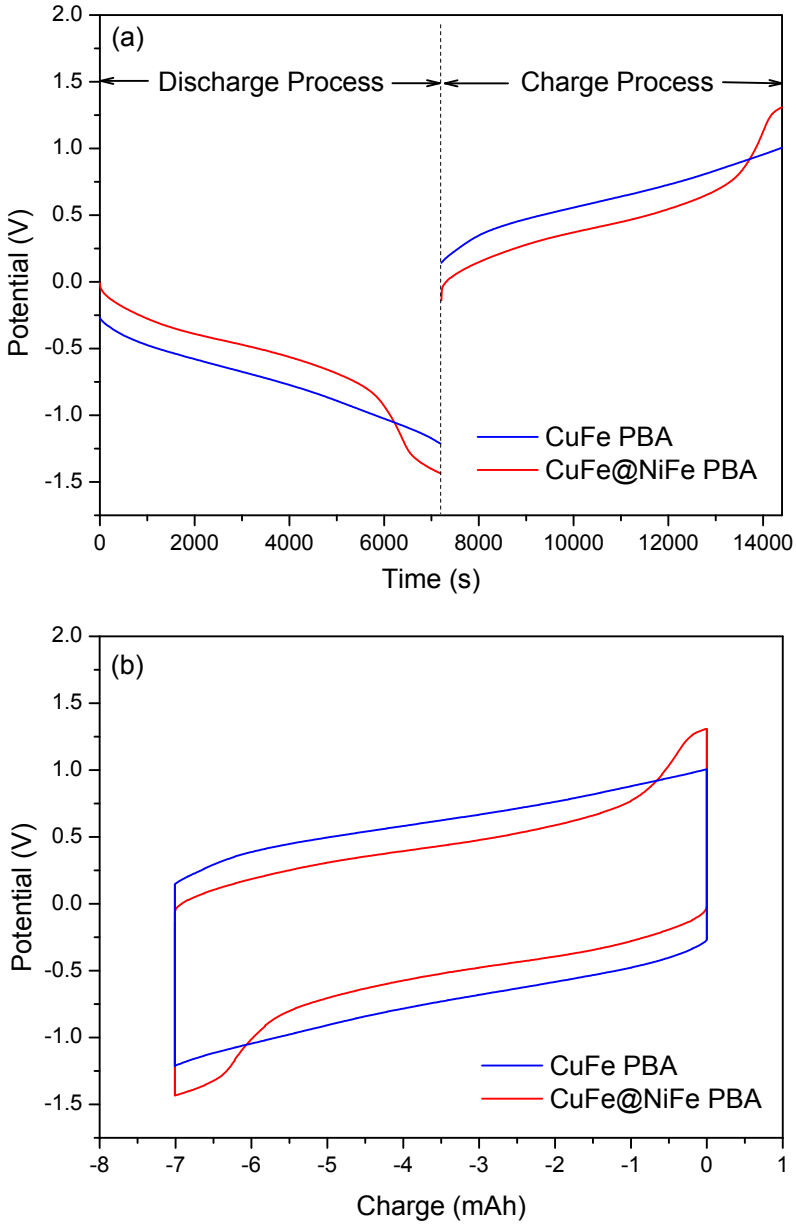

Fig. S7. Voltage change profiles of CuFe PBA cell and CuFe@NiFe PBA cell (a); Voltage-charge profiles of CuFe PBA cell and CuFe@NiFe PBA cell (b).

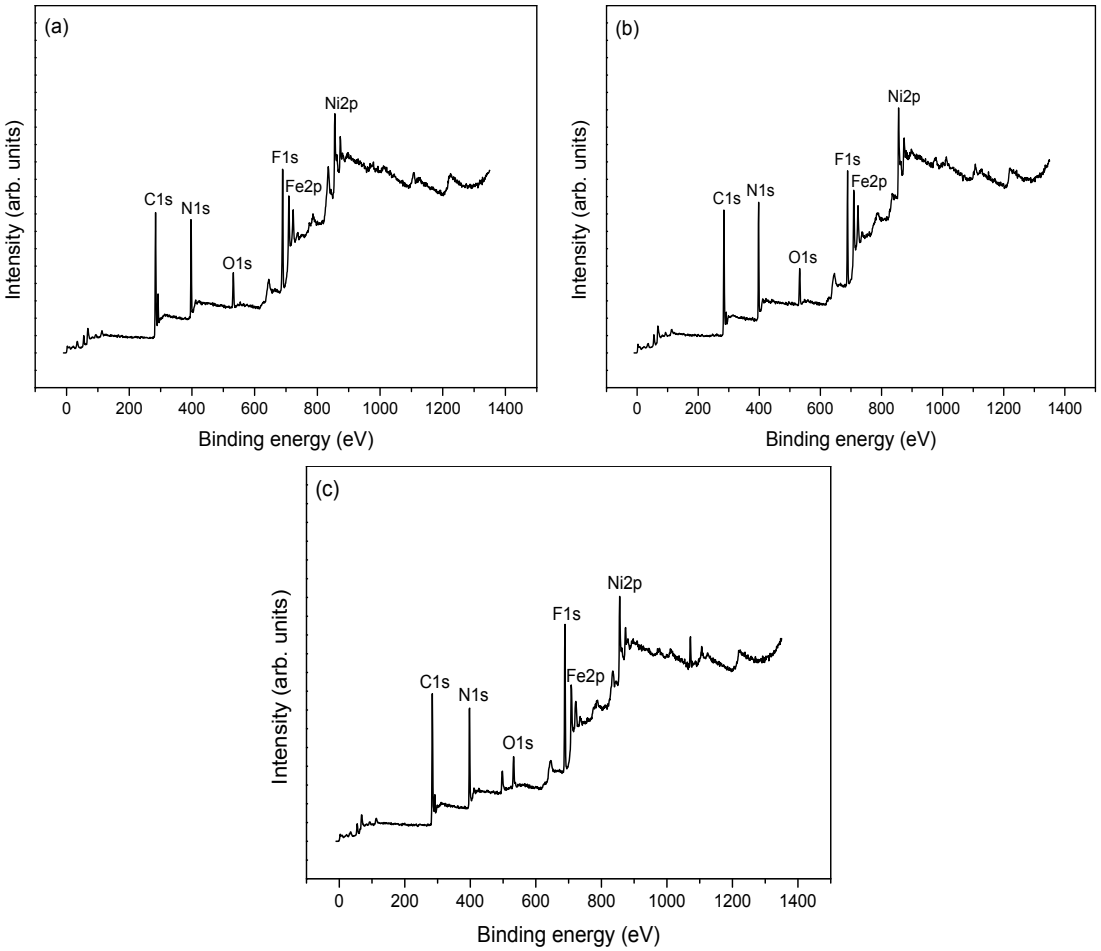

Fig. S8. Survey XPS spectra of CuFe@NiFe PBA electrode at the beginning of the first cycle (a), the end of the first discharge period (b), the end of the first charge period (c).